LA-1479
C. 6.3

CIC-14 REPORT COLLECTION
REPRODUCTION
COPY

LOS ALAMOS SCIENTIFIC LABORATORY

OF THE

UNIVERSITY OF CALIFORNIA

CONTRACT W-7405-ENG. 36 WITH

U. S. ATOMIC ENERGY COMMISSION

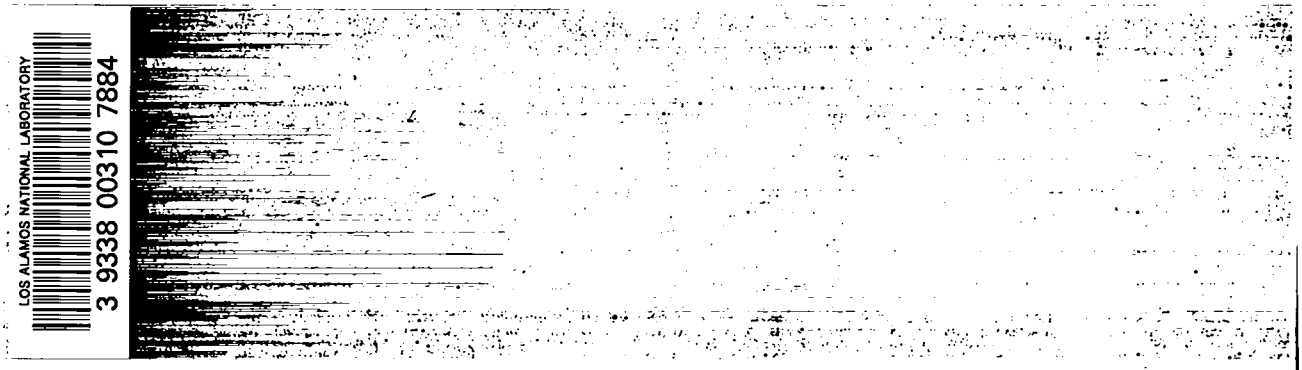

c.16

LOS ALAMOS SCIENTIFIC LABORATORY
of the
UNIVERSITY OF CALIFORNIA

Report written:
October 1952

LA-1479

Report distributed: JAN 19 1953

ABSOLUTE CROSS SECTION FOR THE REACTION $T(d,n)He^4$ FROM 10 TO 120 KEV

Work done by:

W. R. Arnold
J. A. Phillips
G. A. Sawyer
E. J. Stovall, Jr.
J. L. Tuck

Report written by:

W. R. Arnold
J. A. Phillips
G. A. Sawyer
E. J. Stovall, Jr.
J. L. Tuck

LOS ALAMOS NATL. LAB. LIBS.
3 9338 00310 7884

PHYSICS

ABSTRACT

The cross section for the reaction $T(d,n)He^4$ over the low-energy range from 10 to 120 kev has been measured at about 90 points by an absolute method. This method used a deuteron beam passing into a thin tritium gas target; the alpha particles from the reaction were observed at 90^o in the laboratory system. The total cross sections obtained, assuming isotropic distribution in the center of mass system, show a peak of 4.95 barns at 107 kev deuteron energy.

The probable error in these measurements is estimated at $\pm 3\%$ at 100 kev, 3.5% at 25 kev, 10% at 10 kev. A Gamow plot with the theoretical slope passes through the measured points at 20 and 16 kev. This leads to the relation

$$\sigma(\text{barns}) = \frac{2.26 \times 10^4}{E} e^{-44.40 E^{-1/2}}$$

with E the deuteron energy expressed in kev. For cross sections below 16 kev, this relation is preferable to the experimental values since systematic errors could be large.

ACKNOWLEDGMENT

We acknowledge with pleasure the assistance of the following:

E. Fermi and R. L. Garwin, who called the problem to our attention and had an important share in formulating the experiment;

H. Agnew, who contributed to the design of the apparatus;

W. Ogle, who suggested the deceleration technique;

J. H. Coon, who designed the tritium handling apparatus and advised in this field;

B. B. McInteer, who provided the mass spectrographic analysis.

I. INTRODUCTION

The $T(d,n)He^4$ cross section had been measured at energies below 150 kev deuteron energy several times previous to the fall of 1950,[1,2] but the results did not agree. The measurement of this cross section presents several problems which are peculiar to the low-energy range. These may be summarized as follows:

(a) σ is a steep function of energy. At 20 kev, a 100 volt change in energy causes a 2% change in cross section, while at 10 kev, 100 volts of change cause a 6% change in cross section.

(b) The stopping power of most substances passes through a maximum in the region of 50 to 100 kev deuteron energy so that, combined with (a) above, even monatomic layers of contamination on targets can introduce significant error.

(c) At the time these considerations arose (1950) the stopping power for likely target materials was certainly not known to within $\pm 20\%$ at these low energies.

(d) The cross sections for the charge exchange reactions

$$D^+ + X^O \rightarrow D^O + X^+$$

and

$$D^O + X^O \rightarrow D^- + X^+$$

become large when the velocity of the beam deuteron approaches the velocity of an orbital electron, which is the energy range of the present experiment. The charge exchange cross section approximates molecular dimensions ($10^{-16} cm^2$). Thus the beam current measurement can be complicated by exchange with the normally negligible residual gas in high vacua.

In planning this experiment, it seemed that thick target methods were ruled out by (c) since in such cases

$$\sigma = dY/dE \cdot dE/dx$$

On the other hand, thin targets can be made so that the error introduced by an uncertainty in dE/dx by, say, 20% introduces an inappreciable error. This calls for a target density in the region of $10^{-5} gm/cm^2$ and in such a case we obtain the cross section

$$\sigma = N/n_1 n_2 \ell \Omega$$

where

N = number of disintegrations

n_1 = number of bombarding particles from the beam current

n_2 = target density in particles/cm^2

ℓ = beam path length in the target

Ω = the counting system solid angle

While it is perfectly possible to obtain films of tritiated ice or tritiated zirconium of sufficient thinness, the problem of estimating n_2 in such films seemed unattractive for an absolute experiment and, in addition, back-scattering of particles from the support which such films require is a further complication.

A thin target consisting of several centimeters of path in gas at 1 mm pressure seems ideal for precise determination of n_2 and ℓ, n_2 being defined by the readily measurable gas composition, pressure, and temperature, and ℓ being large enough for direct measurement.

Such gas targets are commonly operated by admitting the beam through an aperture from the high vacuum region and disposing of the outflowing gas by a fast differential pumping system. However, at the low energies reason (d) rules against this; the pressure in the antechamber, combined with the large charge exchange cross section, makes the beam current measurement untrustworthy. Some workers[2] have avoided this difficulty by abandoning measurement of beam current, and have measured beam power calorimetrically.

The solution adopted here has been to interpose a thin window between the gas target and the high vacuum. The problem then becomes one of knowing the energy loss in this window with sufficient accuracy, and correcting for the scattering and straggling in the beam produced by it.

Although in principle it is possible to correct for any degree of scattering and straggling, such corrections impair the reliability of the results, and in designing this experiment the aim was to keep the total magnitude of such corrections below the planned probable error of 6%. The requirement that the scattering correction be less than 6% proved to be equivalent to the requirement that half the beam be included within an angle of 5°, or for 20 kev deuterons in window material with an atomic number in the region of 13(Al), a thickness of $10\,\mu g/cm^2$. The straggling correction depends on the curvature of the σ vs E curve, and is most serious at the lowest energies. We find from the measured σ vs E curve that at 20 kev, if $\Delta\sigma$ is the error, $\frac{\Delta\sigma}{\sigma} = 0.4\delta(E)/E$ where $\delta(E)$ is the root-mean-square deviation in the straggling. Hence $\delta(E)$ must be < 3 kev for a correction $<6\%$.

It proved possible to develop windows fulfilling these requirements. They consist of evaporated films of SiO, thickness about 7 $\mu g/cm^2$ (not known precisely), capable of withstanding 1 mm gas pressure on a diameter of 8 mm, of substantial durability under bombardment by 1 μa of deuterons, and with sufficient constancy in thickness. A characteristic film has a mean energy loss of 5 kev at 30 kev, straggling ± 0.7 kev, and average scattering angle of 5°. The films are reported elsewhere.[3]

The beam current is determined by measuring the charge accumulated by the target chamber and window as a whole. The beam defining apertures and guard rings are main-

tained in a high vacuum so that the guard rings can be effective and the charge exchange small.

Other considerations taken into account in the experiment were:

Error in the target density, n_2, produced by:

(a) Temperature differences between manometer and target chamber.

(b) Local change of gas density produced by heating caused by passage of the beam or by contact with the hot window. This effect might be detected by an apparent change of σ with beam current. None was found.

(c) Repassage of beam particles through the target volume caused by back-scattering in the rear of the chamber. This latter turns out to be negligible on account of the combination of steep fall-off of σ with E, and the small angle subtended by the target volume, from the rear of the chamber.

II. EXPERIMENTAL PROCEDURE

1. High Voltage Supply and Measurement

In making this measurement of the T-D cross section the deuterons were accelerated and the tritium gas was used in the target because at the maximum high voltage of the accelerator (130 kev) a higher reaction energy could be reached than if tritons had been accelerated.

The high voltage, supplied by a conventional Cockcroft-Walton voltage doubler (described by Bretscher[4]) was fed through a surge resistor to a box containing the probe and focus voltage supplies. The center of the two-gap accelerating tube was tied through surge resistors to the half voltage point. The apparatus is shown schematically in Figs. 1 and 2.

The high voltage was measured by means of a series of 30 high voltage resistors (Shallcross Type 505) of 5 megohms each, rated at 7.5 kv each. The total resistance of the resistors was measured in the Los Alamos Standards Laboratory and fell well within the 0.1% accuracy specified by the manufacturer. A 1000-ohm standard resistor was placed in series with the high voltage stack, at the ground end, and the potential across it measured with a type K potentiometer.

The linearity of the high resistance stack was checked by the following method. An identical stack was placed in parallel with the high voltage stack, and used as an indicator to hold the high voltage constant. The current through the standard stack was measured; then the top half was shorted out and the current checked to see if it had doubled as required. The procedure was repeated, shorting out the bottom half. The deviation from linearity was less than 0.05%. During these tests the voltage gradient down the standard stack was twice

the maximum expected while operating and, since there was no deviation from linearity, no corona down the stack was to be expected at the operating gradient. The standard stack was also run for almost an hour at twice the maximum wattage dissipation of the parallel stack, and twice the maximum dissipation expected during operation. No drift of resistance was observed.

The top of the high voltage measuring stack was connected to the anode of the ion source (which potential was closest to that of the ions). The ions start out at a potential slightly below this, and the correction for this is discussed under 'Energy of Beam in Target' (Section 2 below).

The ripple on the high voltage, with all parts of the apparatus functioning, was calculated to be 1 volt/kv. A measurement with condenser and oscilloscope gave about 5 volts/kv, but this must be considered an upper limit on the ripple since there was some pickup from the high voltage transformer when the measurement was made. A check of the two sides of the analyzed beam spot indicated about 3 volts/kv. Such a ripple introduces an error in the cross section proportional to the curvature of the E vs σ characteristic. For a ripple of 5 volts/kv, the error in σ is $<0.1\%$ at all energies and was neglected.

The high voltage was held constant manually by adjusting a vernier variac in the high voltage a-c supply so as to hold the potentiometer (across the 1000-ohm standard resistor at the bottom of the high voltage resistance stack) in balance. With this system it was possible to hold the drifts in the high voltage to less than 50 volts, provided their period was longer than the 2 sec period of the balance galvanometer. Shorter period fluctuations were rare and their duty cycle was too short to cause any effect on the cross section. The minimum observable change in high voltage with this system was 5 volts.

2. Energy of Beam in Target

The energy of the ion beam in the target chamber differed from the energy represented by the high voltage measurement because of (a) a small voltage drop ($\sim$100 volts) between the ion source anode and the ion plasma in the ion source, and (b) a much larger loss of energy ($\sim$5 kv) in the thin window of the target chamber. A decelerator was used to measure the energy of the ions after they passed through the window, and hence to measure both voltage drops.

A gate valve at the rear of the target chamber could be opened when the chamber was evacuated to allow the beam, degraded in energy by the thin window, to pass into the decelerating gap of the decelerator of Fig. 2. In order to avoid having two high voltage supplies, and two accurate voltage measuring devices, the same high voltage that accelerated the deuterons was led over through an X-ray cable to the decelerator. Since the deuterons of

the beam had lost some energy, this voltage was too high and had to be reduced an amount ΔV equal to the amount of energy lost in the film) before the deuteron was able to reach the collector of the decelerator. This differential voltage, ΔV, was supplied by an auxiliary power supply mounted in a box at the high potential. The voltage, ΔV, of this power supply was measured by six high voltage Shallcross resistors and a microammeter. This voltmeter was calibrated against the standard voltmeters of this Laboratory.

In operation, deceleration curves such as those in Fig. 3 were obtained. The 'no foil' curve shows that the energy spread of the beam was about 100 volts, and the average energy of the ions about 100 volts below the high voltage reading. Since these amounts were included in the deceleration curve which was obtained with an SiO window in place, they were included in the differential voltage, ΔV, subtracted from the high potential to obtain the energy of the ions in the target chamber, and were of importance only if they changed between a deceleration and a run. The constancy of these ion source drops was checked carefully and found to be a function only of the ion source gas pressure, which was held constant during cross section measurements.

The type of deceleration curves obtained with an SiO window is shown to the right in Fig. 3. This foil had an average thickness of 3360 volts, along with straggling or half width of about 750 volts. The fact that the straggling is a large fraction of the total energy loss can be explained on the basis of the statistics of the number of interactions of an ion passing through a film only 100 atoms thick. Fifty interactions with an average energy loss per interaction of around 90 ev would give the observed straggling.

This interaction energy, which is rather large compared with the energy required to produce an ion pair (32 ev), has been predicted on degeneracy grounds at low energies.[5]

During a deceleration of the positive ions in the measurement of the thickness of a foil, any negative ions caused by charge exchange in the window would, of course, be accelerated. Thus when the voltage on the decelerator was such as to collect no positive ions, the reading on the electrometer would be an indication of the number of negative ions. The small negative current observed was assumed constant throughout the deceleration since there was no change in the electrometer reading as the deceleration voltage was varied (except when positive ions were being collected).

Although charge equilibrium had undoubtedly been reached in the window, there was a possibility that the negative ions did not have the same energy distribution as the positives. This doubt was removed by running the machine at low incident voltages, reversing the polarity of the voltage supply in the decelerator, and decelerating the negative ions. When corrections were made for the biasing voltages on the guard rings, the loss of energy in passing

through the foil for both positive and negative ions was found to be the same.

Because of the geometry of the decelerator only the central component of the beam was decelerated. However, it is believed that the increased energy loss of the more widely scattered deuterons (caused by a greater window thickness traversed) was small because the path length in the window varies only as the secant of the scattering angle. Also, since both oxygen and silicon are so much heavier than the deuterons, the energy loss per scattering event is small. At the lowest energies the error introduced was about 2%.

The energy loss of SiO windows as a function of energy was measured carefully, and this variation with energy is shown in Fig. 4. Thus, although a given series of runs was made at a variety of energies, it was only necessary to decelerate at one energy before and after the series to be able to calculate the energy loss at other energies.

Since the thickness of the window changed with time as a beam traversed it, it was necessary to make a linear interpolation of the thickness with time during a run.

The cross section varied so rapidly with energy that it was necessary to keep the total window growth during a run to about 500 volts in order that the interpolation could not introduce an appreciable error. The growth of the SiO windows appeared to be due to the deposition of carbon derived from condensable vapors in the system. The windows, although growing by the decomposition of oil on their surfaces (a process about four times as fast with gas behind the window as in a vacuum), were also losing material due to the bombardment. With beams of over a microampere the films often got thinner with running time.

It is interesting to note that, since SiO is an insulator, the window gains positive charge by exchange with the incident deuteron beam. If this charge remains unneutralized, a potential builds up and the incident particles are decelerated upon approaching the window, pass through the window with a reduced energy, and are accelerated upon leaving. At these energies the smaller the energy of the beam particle, the smaller the loss of energy that it suffers upon passing through the window. Because the deuterons lost about 100 volts less when the window was charged than when discharged, by reference to the curve of ΔE vs E, Fig. 4, it was estimated that the window charged up to about 2 kv.

Although the target was thin, the energy loss of the deuterons in passing through the gas from the window to the axis of the collimators was large enough to need a correction, especially at the lower energies. dE/dx values measured with the decelerator were used to make this correction[6] (Fig. 5). The energy loss in the gas target was about 300 volts.

3. Ion Source

One of the difficulties in using a mass 2 beam of deuterium is that it may be contaminated with some molecular hydrogen beam; the amount depending on the purity of the deuterium

gas used, and the ratio of atomic to molecular beam produced by the ion source. Since a very high atomic to molecular ratio is obtained from an rf type ion source, one of these was used. The design was copied from the Oxford source.[4] The atomic to molecular ratio of this ion source was greater than 10, and since there was less than 1% hydrogen in the deuterium supply gas, the amount of molecular hydrogen in the atomic deuterium beam was less than 0.1%. Also, since the rf source is fairly efficient, it was possible to use very low gas flows through the ion source and still obtain adequate beams (0.1 to 1 μa). Larger beams could not be used because they destroyed the SiO windows. This resulted in lower pressures in the accelerator tubes and hence lower neutralization percentages. Neutralization and molecular contamination of the beam are discussed below under 'Beam Measurement' (Section 8 below). The ion source consumed about 1cc/hr of deuterium. The probe voltage, which draws the ions out of the plasma, was about 1 kv. About 200 watts of rf power were used.

4. Vacuum System

After passing through the probe channel of the ion source, the beam passed through two focusing gaps used to obtain the desired diffuse beam on the target chamber window. It then proceeded through two accelerating gaps to an analyzing magnet which deflected the desired mass 2 beam through 30^{o}. The operating pressure in this part of the system ran at about 12×10^{-6} mm Hg. The beam then passed through an 8 in. section of 3/4 in. diameter tubing held at liquid air temperatures, and with 3/8 in. diameter diaphragms at each end. This liquid air trap removed condensable vapors near the window. The beam then emerged into the 'clean' part of the apparatus where great pains were taken to eliminate, as far as possible, sources of condensable vapors which would lead to an increase in the thickness of the target chamber window. Lead gaskets were used in this region instead of neoprene O-rings. A side arm pumping system was also used at this point to reduce the pressure to 4×10^{-6} mm Hg and thereby reduce the amount of beam neutralization.

5. Target Chamber

The target chamber is shown in detail in Fig. 2. The beam is shown entering at the right through the deflecting magnet (used to measure neutralization), the 5 mm diameter collimating hole, and the electron suppression electrode. The beam then impinges on the 8 mm diameter entrance window of the target chamber. At the left the target chamber was closed by a vane type valve which could be opened to admit the beam to the decelerator. Glass insulators were used to insulate the target chamber from the accelerator tube and decelerator while thin mica rings insulated the target chamber from the counters. The target chamber was insulated so the beam current to it could be measured.

6. Target Atoms

Since a gas target was used, the calculation of the number of target atoms per cm^3 depended upon measurement of pressure, temperature, and purity.

A. Pressure. Measurement of pressure was complicated by the requirement that condensable vapors in the target chamber be kept to an absolute minimum, for reasons that will be discussed below under 'Purity.' This ruled out the use of oil or mercury manometers in direct contact with the tritium gas in the target chamber. Instead, a Consolidated Engineering Company micromanometer was used to measure tritium gas pressure. The micromanometer was not absolute and had to be calibrated with a fluid manometer.

The micromanometer has a diaphragm which is deformed by the pressure to be measured, changing the capacity between the diaphragm and a fixed plate. This capacity is in one arm of a capacity bridge which may be balanced by placing a standard variable condenser in another arm and adjusting to balance. The drift in zero pressure capacity was reduced to acceptable limits by immersing the gauge proper in an oil bath whose temperature was held constant to $0.1^{\circ}C$.

The fluid manometer used for calibration consisted of a U-tube constructed of 1 cm bore precision glass tubing. Collimated light from two sources striking the respective menisci was viewed by two microscopes mounted on a vertical cathetometer. The cross hairs were set on the first dark line of the diffraction pattern produced at the fluid-air interface and the setting was very reproducible. The calibration of the gauge was checked periodically throughout the series of runs and did not vary by more than $\pm$ 0.3% throughout. It was necessary to calibrate at the end of a day's running so that the manometer vapor introduced into the gauge during calibration could be pumped out overnight. Analytical quality butyl phthalate was used as the manometer fluid and, as a precaution against errors of composition, its density was measured over a range of temperatures with a standardized pycnometer.

The accuracy of the pressure measurement is estimated to be 0.5%, of which 0.2% is the error in calibration with the oil manometer.

B. Temperature. Two measurements were made: (a) the temperature of the target chamber body as read by a thermometer, and (b) the temperature difference between the gas and the chamber body as measured by a fine wire thermocouple in the gas. The latter was discarded after no temperature difference was observed between gas and chamber body.

C. Purity. Attainment of purity proved to be one of the major difficulties in the experiment. Tritium was supplied from a small uranium reservoir, and after use was collected into another uranium trap. About one third of the gas from each filling was taken as a sample for analysis. The tritium gas was analyzed on a mass spectrometer before and

after use. However, the gas sample was collected at about 800 to 1000 dynes/cm^2 (about 2/3 mm Hg) and then compressed by a Toeppler pump to 1 cm Hg during the mass analysis. This meant that a condensable vapor might not have been detected. One check on condensable hydrocarbons was to look at the CT_4 mass spot in the mass spectrometer, since CT_4 would be formed from hydrocarbons in an ionized tritium atmosphere. Very small amounts of CT_4 were observed, but there was no way of getting a quantitative check on hydrocarbons.

The method used for condensable vapors was to try to eliminate rather than measure them. It was found during the first runs that the measured yield fell, with time, about twice as fast as could be accounted for by growth of the target window, and was frequently an erratic function of pressure changes caused by adding or removing part of the tritium. The difficulty was apparently due to an increase in the partial pressure of oil vapors which started building up the moment the target chamber was isolated. Such a rise in pressure could be noted on the Consolidated gauge and was much worse immediately after calibration (which involved exposing the systems to fluid vapors).

The pressure rise was reduced to less than 0.3 dynes/cm^2/min at pressures of less than 5 dynes/cm^2 in the target chamber by pumping at least overnight after calibration. Although this rate of rise extrapolates to predict a 2% drop/hr in cross section, the drop actually observed was in almost all cases less, indicating that vapor evolution was retarded by the presence of the tritium, or else reached an equilibrium pressure.

The gas entered the target at 99.5% tritium plus 0.5% hydrogen, and the mass analysis after running was usually about 96% T, 2% H, 2% N. The absence of oxygen to go with the nitrogen indicated that air had entered the chamber during the run instead of during handling of the sample, and that the oxygen had been converted to T_2O in the ionized target gas. The T_2O could not be measured on the mass spectrometer because of background difficulties. However, water vapor (T_2O) was not a cause of error since the number of tritium atoms per unit pressure is the same as for T_2 gas. The increase in hydrogen is undoubtedly due to exchange with hydrocarbons on the chamber walls. At very low deuteron energies (below 20 kev) the rate of hydrogen contamination of the tritium was greatly increased, possibly due to widely scattered beam particles striking the gelva (polyvinyl acetate) used to anchor the collimator slits in the collimator tube. This is one of several factors which decreases the accuracy of these very low energy measurements.

The inaccuracy in the cross section introduced by change in tritium purity is estimated at $\pm$ 1% at energies above 25 kev. At the lower energies it is a little higher.

7. Thin SiO Window

The foil window at the entrance to the target chamber served to contain the target gas and to admit the deuteron beam to the target chamber.

The SiO windows used in the experiment were 5-10 $\mu g/cm^2$ (about 100 atoms thick) and were made by evaporating SiO onto a thin zapon backing which was later removed by bombarding the film in the ion beam of the accelerator. The SiO films have been discussed more fully elsewhere.[3] The windows were glued to their holders with dextrose; dextrose was used because it is a low temperature thermoplastic which is insoluble in zapon solvents. The windows had to be strong enough to withstand the gas pressure in the target chamber and the deuteron beam, and at the same time thin enough not to cause large energy loss, straggling, or angular divergence.

As mentioned previously, SiO windows become positively charged when a beam is passed through them in a vacuum because of charge exchange with the incident beam. This charging leads to electrostatic forces strong enough to rupture the film. During the deceleration operations, a small tungsten filament (from a flashlight bulb) behind the window in the target chamber was heated to supply enough electrons to keep the window neutralized. With gas in the target chamber, there is a sufficient amount of ionization in the gas to discharge the window so the filament is then not heated.

Aluminum foils were used originally but discarded because the beam apparently causes the aluminum to react quite rapidly with the residual oxygen in the vacuum, leading to a rapid increase in thickness of the foil with time. SiO grows at less than half the rate of Al.

8. Beam Measurement

In the design of this experiment all particles incident upon the thin window passed through target gas which was visible from the proportional counters. Thus the whole target chamber could be made a Faraday cup, and the chamber was insulated for this purpose. In order for the current measured to the target chamber to be translated into incident particles, the following precautions had to be observed.

A. Conduction between chamber and ground was made negligible by good insulation. Other sources of error were: (1) electrons knocked out of the window by the incoming beam, and (2) escape of deuterons by back-scattering.

An appreciable electron current due to (1) was found and was suppressed by a negatively charged electrode between window and beam defining slit. The potential required to suppress the current was proportional to the energy of the incoming beam; 1 volt of suppression per kilovolt of beam energy reduced it to zero. Deuterons scattered from the window or

through the window from the interior of the target chamber were not suppressed and, by calculation, should be quite negligible.

B. No extraneous charges shall reach the target chamber. Undesired parts of the incoming beam were removed by the 5 mm defining slit, the edges of which were sharp enough so that there should have been no appreciable scattering at these energies. Another source of spurious charge was selective collection of ions produced by the beam in the residual gas of the vacuum outside the window. The target chamber was held 10 to 16 volts positive with respect to ground by the current integrator and hence could collect negative ions from this region. However, the electron suppression electrode was 100 to 150 volts negative, and could collect positive residual gas ions from the same regions, so that the positive current to it gave an indication of the error from this source. The error was quite negligible.

C. Corrections for neutralized deuterons in the beam. A fraction of the beam incident on the target was neutral due to charge exchange with the residual gas between the analyzer magnet and the target chamber and gave reactions although not registering as charge. These reactions were estimated by the following procedure: the incident beam was adjusted so as to be as steady as possible and three runs were made. The first and third were made with both charged and neutral particles entering the target, while the second was made with the charged particles being deflected by a neutralization magnet placed directly in front of the SiO window so that only neutrals entered the target. From the data for these three runs the percentage of neutrals was calculated. The accuracy of the measurement of the percentage of neutrals was only 10% but since the neutral beam was, at most, 5% of the charged beam, there was an uncertainty of less than $\pm$ 0.5% in the total number of incident particles. At the lower energies, some negatively charged deuterons were produced, and these, if numerous, could have produced an error in the beam current measurement since the method used to detect neutrals did not indicate the presence of negatives. Measurements of the positive-neutral-negative ion proportion as a function of energy, made in another apparatus, show that the energies do not go low enough in these correction measurements for the negative ions to reach significant proportions.

D. Beam contamination. For most of the data the mass 2 beam spot was used and contamination of the D^+ ions with H_2^+ had to be considered. However, as discussed previously, the ion source used produced over 10 times as many atomic ions as molecular ions, and since the deuterium used contained less than 1% hydrogen the H_2^+ should have been less than 0.1% of the mass 2 beam. A check was made by the comparison of cross sections obtained with mass 2 and mass 4 beam; these checked within the statistical error of 1.5%.

E. Current integrator. The current integrator used has been described else-

where.[6] It is not absolute, and so was calibrated with a potentiometer and a standard resistor. Calibrations had an internal consistency of 0.3%. The absolute accuracy appears to be 0.5% for currents above 0.04 μa.

9. Counters

The number of reactions taking place was determined by counting the alpha particles from the T-D reaction. With a well-defined beam passing through the target chamber and a collimated counting system, the solid angle seen by the counters could be calculated precisely. In this experiment it was assumed that the alpha particles were given off isotropically in the center of mass system, based on the results of Bretscher and French.[1]

The counters used to detect the alpha particles from the reaction were argon-filled proportional counters, 2 in. diameter and 6 in. long, with a 2 mil central wire. Mica windows of 1 in. diameter and 1.5 mg/cm^2 thick admitted the alpha particles to the counters. Below the counters were collimating slits which limited the area of the counter window used. The counters were filled to 10 cm pressure with argon and operated with 550 volts on the center wire.

Counter pulses from each counter were recorded separately with a Los Alamos Model 101 amplifier and a Model 750 scaler. Amplifier gain was set to make the alpha pulses from the T-D reaction 50 volts high. Variation in pulse height of the alpha pulses was about 10%.

The alpha counting rate was constant, within the 2% statistics, from 0 to 40 volts discriminator setting, indicating that all pulses were counted at the chosen discriminator setting of 20 volts. At a counting rate of 1000/sec counting losses caused by the insensitive time of the amplifier after a pulse amounted to 0.2%. Accordingly, counting rates were always kept below 1000/sec.

Background of the counters was about 1 count per 100 sec and was therefore negligible. A shutter was provided at the counter window which would stop the alpha particles but admit neutrons and with the shutter it was determined that T-D neutrons did not cause counts in the counters.

10. Solid Angle and Path Length

The length of the paths of the deuterons in the target volume, and the solid angle of acceptance of the counters at different points along the path, vary with the inclination and orientation of the beam path. It is first necessary to know the angular distribution of the beam as scattered by the window. This was measured by building an apparatus in which an arm with a small shielded Faraday cup rotated about the center of the window as an axis. The current collected by this cup as a function of scattering angle θ gave data of the type shown in Fig. 6. A series of such curves taken at various energies was translated into curves showing how the

percentage of beam current included inside a given angle varies with energy (Fig. 7).

In these measurements, the angular resolving power was of the order of 1.2^{o}, and an unscattered beam would have had an angular half width at half maximum of 1.1^{o}.

In order to apply these scattering measurements to the solid angle correction, it was necessary to construct a universal curve from which the divergence produced by windows of differing thicknesses could be read off at various energies.

It was found experimentally that the data could be well represented by a universal curve in which intensity was plotted against $\frac{E}{\Delta E^{1/2}}\theta$ where ΔE is the energy loss in the film measured at a standard 30 kv energy, and therefore a measure of its thickness, and E is the average deuteron energy in the window.

The above scaling coefficient would be in accord with a predominantly multiple scattering in these windows. However, calculation shows that in fact the scattering must be mainly single, with plural scattering for the least scattered one third of the transmitted beam. At these low energies, the penetration of the scattered nucleus into the scattering atom is small, so that screening is important. We have attempted to calculate the distribution of the scattering from a film of 10^{17} SiO molecules/cm^2, using a Thomas-Fermi field for Si and O, and the scattering theory of Moliere.[9] This gives a half width for the scattered beam of only about 40% of the observed value, and departures from a gaussian distribution, especially at large angles. It is doubtful that the discrepancy could be wholly accounted for by an underestimate of the film thickness, and carbon deposits do not affect the scattering very sensitively. It has been suggested (H. Bethe, private communication) that at these low energies the simple coulomb scattering may be complicated by quantum mechanical effects.

In applying the universal scattering curve to the correction, for counter solid angle, the approximation was made that the distribution could be represented by scattering at three angles, θ_1, θ_2, and θ_3, each containing one third of the total beam (this approximation is considerably better than needed to keep within the desired accuracy). From the curve in Fig. 8, one finds that

$$\theta_1 = 33(\Delta E)^{1/2}/E$$
$$\theta_2 = 71(\Delta E)^{1/2}/E \text{ and}$$
$$\theta_3 = 137(\Delta E)^{1/2}/E$$

Thus for any given run, knowing ΔE, the energy loss in the window at 30 kev, and E, the mean beam energy in the window ($= E + 1/2\,\Delta E$), three average angles representing the scattering could be calculated.

The next step is to calculate the average solid angle and target path length as a function of θ, the divergence.

Using the geometry of Fig. 9 and the measured slit data of Table I, the value of Ω can be calculated algebraically for points on any particular ray, of inclination to the axis θ and azimuthal angle α , as a function of distance along the ray, ℓ. Fig. 10 shows such Ω plotted against ℓ for three inclinations, $\theta = 0^{\circ}$, 10°, 20°, and $\alpha = 0^{\circ}$, and 180° (corresponding to going toward one counter and away from it). Similar curves were prepared for oblique pencils, $\alpha = 45^{\circ}$ and 135°, and $\alpha = 90^{\circ}$. By summing the areas over $\alpha = 0^{\circ}$, 45°, 90°, 135° and 180°, and averaging for the two counter slit systems (which differed by mechanical tolerances), an average value of $\Omega\ell$ could be obtained for a given value of θ. Figure 11 shows the resulting $\Omega\ell$ averages as a function of θ.

It turns out that this geometrical factor $\Omega\ell$ is insensitive to θ over the range zero to 30°, varying only 2%. At $\theta = 32^{\circ}$, $\Omega\ell$ jumps by nearly 10%, and this occurs when particles pass inside the counter slit system. In these experiments few particles were scattered out to $\theta = 32^{\circ}$. From Fig. 7, at 20 kev we see that in one particular case 99% of the beam lay within $\theta = 25^{\circ}$ for beam energy 20 kev.

These linear approximations to nonlinear functions used in calculating the effect of scattering were more than sufficiently accurate since the whole correction to $\Omega\ell$ because of scattering is only 1% and the uncertainty in $\Omega\ell$ due to other factors is larger. The corrections are included in this report mainly because it was not immediately obvious that the correction for divergence would be so small.

The error in calculation of the solid angle is about 0.5%, while errors in slit width and position may introduce errors of 0.3%. An error of 0.3% may be introduced by a non-homogeneity of the beam causing a much larger fraction of the deuterons to go through the upper half of the window than through the lower half. Since the non-homogeneity factor always increases the solid angle, the total error on the solid angle factor is set at 2%.

III. DATA AND CALCULATIONS

Table II is a sample data sheet which shows how the data were taken in the experiment. This set of data was taken from the twenty-second filling of gas, for the first two of several energies, and was selected at random. Tables III through V show the calculations leading from the data of Table II to final cross section values. Table III was calculated from Table II plus the data of Fig. 3. The interpolation of foil growth is linear through the run. The thicknesses of foil at the 85 kev incident deuteron energy were obtained from Fig. 4 using the 25 kev incident figures. Table IV gives the calculated product of solid angle times path length obtained by the method outlined under 'Solid Angle and Path Length' (Sect. 10, above). Table V then gives the calculations leading to the value of the absolute cross sections. The tritium

purity was interpolated linearly with time. This is only an approximation, since the experiments indicated that the drop in T purity was much greater at lower energies. The explanation is that the more widely scattered beam at lower energies caused a greater amount of exchange with wall contamination. The effect was appreciable only below 20 kev where a different method of calculation of T purity was used to compensate for the additional problem of condensable vapors: runs at 40 kev at the beginning and end of low energy runs were used to obtain the total percentage drop in yield due to T contamination, and a linear interpolation was used between. Another method used to show discrepancies was to take a series of runs at the same energy and check the drop in yield against the drop in T purity.

IV. RESULTS

The experimental values for the cross section are listed on Table VI and shown in Fig. 12 with a smooth curve drawn through most of the points. The peak of the cross section curve, around 107 kev, is quite broad. The experiment did not go very far down the high energy side of the curve due to the limitation of the high voltage and thus accuracy in selecting the peak energy is somewhat limited. The smooth curve of Fig. 12 lies above the experimental points at the energies 7, 9, and 11 kev because failure of the counter collimating system and excess production of condensable vapor gave good reason to expect that the experimental value of the cross sections at these energies might be low. Values used in plotting the smooth cross-section curves at low energies were obtained from the Gamow plot of Fig. 13. The solid line drawn through the points above 20 kev was used to obtain a smoothly varying curve in drawing in the solid line of Fig. 12. The straight line through the points at 16 and 20 kev in Fig. 13 has the theoretical asymptotic value for the Gamow slope.

Table VII gives values for the cross sections obtained from a smoothed curve.

V. ERRORS

An effort was made to keep the errors in the experiment as small as possible. In Table VIII the errors are listed under five headings: number of incident particles, number of target atoms, number counted, solid angle, and energy. Values listed under energy are the errors in voltage translated into error in cross section by using an empirical formula for the cross-section curve. The experiment was designed to go down to 20 kev deuteron energy and, as may be seen from the table, the accuracy falls off rapidly below 20 kev.

The standard error (the root of the sum of the squares) which appears at the bottom of each column was based on the assumption that each of the individual errors is gaussian in its character. Such was most likely not the case, so the error assigned was arbitrarily twice this.

Angular anisotropy in the reaction $T(d,n)He^4$ has not been detected.[1] It is reasonable therefore to assume an s-wave interaction which leads to a cross section with a dependence on energy, at energies remote from the resonance, of the form

$$\sigma = \frac{A}{E} e^{-2\pi e^2/\hbar v}$$

equivalent to

$$\sigma = \frac{A}{E} e^{-44.40 E^{-1/2}}$$

where v is the relative velocity of the nuclei, and the deuteron energy is expressed in kev.

When log $E\sigma$ is plotted against $E^{-1/2}$ (Fig. 13), the points lie on a smooth curve which merges asymptotically into a straight line. The points below 16 kev were neglected and the asymptote through the lowest remaining points, 20 kev and 16 kev, was drawn with the theoretical slope (44.40 barns kev/kev$^{-1/2}$). Since as the energy is reduced, the validity of the theory improves, while at the same time the experimental errors, especially the liability to systematic error, increase, we feel that there is some justification for neglecting the values below 16 kev which fall appreciably below the Gamow theoretical curve.

REFERENCES

1. E. Bretscher and A. P. French, Phys. Rev. 75, 1154 (1949).
2. D. L. Allan and M. J. Poole, Proc. Roy. Soc. A204, 500 (1951).
3. G. A. Sawyer, Rev. Sci. Instruments (in press). Also LA-1077.
4. E. Bretscher, MDDC-1348.
5. E. Fermi and E. Teller, Phys. Rev. 72, 399 (1947).
6. J. A. Phillips, Phys. Rev. (to be published).
7. P. C. Thonemann, J. Moffat, D. Roaf, and J. H. Sanders, Proc. Phys. Soc. 61, 45 (1948).
8. E. Fermi, "Nuclear Physics," The University of Chicago Press, Revised Edition, p. 37, 1950.
9. G. Moliere, Z. Naturforschung 2a, 133 (1947).

Table I

COLLIMATOR SLIT MEASUREMENTS

Slit	Width (cm)	Depth (cm)	Beam to Slit (cm)
Top Collimator			
Inner	2.7 diam*	1.470	1.47
Middle	2.7 diam*	1.463	4.1
Outer	1.458	1.458	6.52**
Bottom Collimator			
Inner	2.7 diam*	1.467	1.47
Middle	2.7 diam*	1.451	4.1
Outer	1.460	1.463	6.52**

* In this dimension at right angles to the beam axis the slit is limited only by the collimator barrel.

**The actual measurement here was between the two outermost slits. The inner slit is the one closest to the beam.

Table II

RAW DATA

Test No.	H.V. (potentiometer volts)	Press ($\mu\mu$f)	Temp (^{o}C)	Integrator counts	Top counter counts	Bottom counter counts	Time	Comment
1 start	0.16667	197.74	32.95	0	0	0	2:57:00	
stop	"	197.66	33.0	20	3,748	3,588	2:58:17	
2 start	"	197.65	33.0	0	0	0	2:59:00	Neutralization magnet on
stop	"	197.65	33.0	0	72	64	2:59:30	Neutralization magnet off
3 start	"	197.64	33.0	0	0	0	3:00:00	
stop	"	197.64	33.0	20	3,470	3,498	3:01:03	
4 start	0.56667	197.62	33.0	0	0	0	3:03:30	
stop	"	197.62	33.0	?	8,728	8,848	3:04:09	Discard, current integrator not read
5 start	"	197.60	33.0	0	0	0	3:04:45	
stop	"	197.57	33.0	4	34,114	35,314	3:05:42	
6 start	"	197.57	33.0	0	0	0	3:06:00	Neutralization magnet on
stop	"	197.56	33.0	0	208	224	3:06:30	Neutralization magnet off
7 start	"	197.56	33.0	0	0	0	3:07:00	
stop	"	197.55	33.0	4	34,090	35,050	3:08:02	

Constants used to convert data:

Incident high volts = 1.500×10^5 times potentiometer reading in volts

C_o on micromanometer = 134.10 $\mu\mu$f

Pressure = 7110 $\Delta C/492 + \Delta C$ = dynes/cm^2

Current integrator calibration = 1.246 μcoulomb/integrator click

Starting purity 99.5% T. Final: 95.8% T; 2.2% H, 2.0% N

Run ended 4:21:30

Table III

CALCULATION OF TARGET ENERGY

Test No.	Incident energy (kev)	Foil thickness before (v)	Foil thickness after (v)	Total growth (v)	Fractional time	Growth fraction (v)	Foil thickness during run (v)	Gas thickness* during run (v)	Target energy (kev)
1	25.00	3360	4070	710	.02	14	3374	236	21.39
3	25.00	3360	4070	710	.06	43	3403	236	21.36
5	85.00	5700	6990	1290	.12	154	5854	356	78.79
7	85.00	5700	6990	1290	.15	193	5893	356	78.75

*From dE/dx measurements by J. A. Phillips.[6]

Table IV

CALCULATION OF SOLID ANGLE

Test No.	Foil t = ΔE (kev)	Exit E* (kev)	θ_1	θ_2	θ_3	$\frac{\Omega\ell}{\theta_1}$	$\frac{\Omega\ell}{\theta_2}$	$\frac{\Omega\ell}{\theta_3}$	Avg. $\frac{\Omega\ell}{}$
1	3.37	21.63	2.80	6.03	11.6	.1860	.1872	.1886	.1873
3	3.40	21.60	2.82	6.07	11.7	.1860	.1872	.1886	.1873
5	5.85	79.15	1.01	2.17	4.18	.1858	.1859	.1864	.1860
7	5.89	79.11	1.01	2.18	4.21	.1858	.1859	.1864	.1860

*Energy after emerging from window.

Table V

CALCULATION OF CROSS SECTION

Test No.	Average** (dyne/cm^2)	Incident charge (coulombs)	Total α counts	Neutral beam (%)	Purity (% T)	Yield *	$K/\Omega\ell$ x10^{25}	σ (barns)
1	726.4	24.92	7,336	4.46	99.4	.3896	2.0240	.0789
3	725.7	24.92	6,968	4.46	99.3	.3707	2.0240	.0750
5	725.2	4.984	69,428	1.29	99.0	19.152	2.0381	3.90
7	724.9	4.984	69,140	1.29	98.9	19.100	2.0381	3.89

*Units: alpha count per μcoulomb-dyne/cm^2, corrected for neutralization and purity

**Corrected to 0^oC

K has the value 3.7909×10^{-26} and was obtained from the following values:

4.802×10^{-10} esu/particle

1.013×10^{6} dyne/cm^2/atm

6.024×10^{23} molecules/mole/atm

22.40×10^{3} cc/mole of gas

2.998×10^{9} esu/coulomb

It was assumed that the angular distribution is isotropic in the center of mass system. Corrections for center of mass motion, omitted here, were used in calculating the data in the graphs. This correction is only 0.5% at 100 kev and decreases approximately linearly below that.

Table VI

TD EXPERIMENTAL POINTS

(Energies Arranged in Order Obtained)

E	σ	E	σ	E	σ
49.95	1.358	78.80	3.920	77.74	3.830
44.00	.9635	78.75	3.911	20.07	.05640
43.52	.9276	49.62	.1359	20.00	.05631
72.20	3.362	49.60	.1355	19.93	.05641
15.54	.01887	30.60	.3024	10.94	.002402
33.81	.4219	30.57	.3003	10.80	.002251
52.57	1.5766	68.80	3.0421	10.76	.002082
24.48	.1359	68.76	3.049	42.13	.8785
61 98	2.4077	39.98	.6832	9.60	.001193
42.90	.9106	39.95	.7043	7.53	.000216
42.80	.8758	59.01	2.1461	9.54	.001166
61.71	2.368	58.97	2.1194	41.97	.8689
24.15	.1229	88.10	4.523		
51.97	1.5432	88.05	4.501		
33.23	.3910	97.86	4.916		
14.97	.01542	97.83	4.905		
70.87	3.2354	107.64	4.968		
42.23	.8501	107.59	4.947		
15.87	.02063	117.48	4.775		
15.80	.02008	117.40	4.823		
24.96	1.393	112.39	4.942		
24.91	1.373	112.36	4.952		
24.89	1.398	102.45	4.960		
24.84	.1402	102.39	4.977		
21.39	.07894	77.80	3.8377		
21.36	.07508	77.78	3.819		

Table VII

CROSS SECTIONS DERIVED FROM SMOOTHED CURVE OF FIG. 13

Deuteron energy (kev)	$E^{-1/2}$	σE	σ (barns)
7.5	0.36515	0.00206	0.000275
8.0	.35356	.00344	.000430
9.0	.33333	.00845	.000939
10.0	.31623	.01804	.00180
13.0	.27735	.1014	.00780
16.0	.25000	.342	.0214
19.0	.22942	.852	.0448
22.0	.21320	1.89	.0859
25.0	.20000	3.59	.144
30.0	.18257	8.34	.278
33.0	.17408	13.0	.394
36.0	.16667	18.7	.519
40.0	.15811	28.9	.723
46.0	.14744	51.0	1.11
53.0	.13736	85.9	1.62
60.0	.12910	131.	2.18
67.0	.12217	189.	2.82
73.0	.11704	245.	3.36
80.0	.11180	314.	3.93
93.0	.10370		4.74
100.0	.10000		4.90
107.0	.09667		4.95
110.0	.09535		4.95
113.0			4.94
120.0			4.70

Below 19 kev: $(\text{barns}) = \frac{2.26 \times 10^4 (\text{barn-kev})}{E_{\text{deut}}\,(\text{kev})} e^{-44.40 E^{-1/2}} \quad (\text{kev}^{-1/2})$

Table VIII

ERRORS

	10 kev (%)	25 kev (%)	50 kev (%)	100 kev (%)
1. Number of incident particles				
a. Current integrator	0.5	0.5	0.5	0.5
b. Neutralized beam	0.5	0.3	0.1	0.1
c. Secondary particles	0.3	0.3	0.3	0.3
d. Beam contaminant	0.1	0.1	0.1	0.1
2. Number of target atoms				
a. Pressure	0.5	0.5	0.5	0.5
b. Tritium purity	2.0	1.0	1.0	1.0
c. Temperature	0.1	0.1	0.1	0.1
3. Number counted				
a. Efficiency of counters	0.2	0.2	0.2	0.2
b. Statistics	0.5	0.2	0.1	0.1
4. Solid angle				
a. Beam not central	0.3	0.3	0.3	0.3
b. Measurement of slit system	0.3	0.3	0.3	0.3
c. Error in calculation approximations	0.5	0.2	0.2	0.2
5. Energy				
a. High voltage measurement	0.6	0.4	0.3	0.10
b. Variation in high volts	1.6	0.4	0.2	0.03
c. Spread in particle energy	0.4	0.3	0.1	0.02
d. Film thickness	3.0	0.7	0.3	0.05
e. Energy loss in T gas	3.0	0.7	0.3	0.05
Standard error:	5.3	1.8	1.5	1.4
Assigned error:	10.0	3.5	3.0	3.0

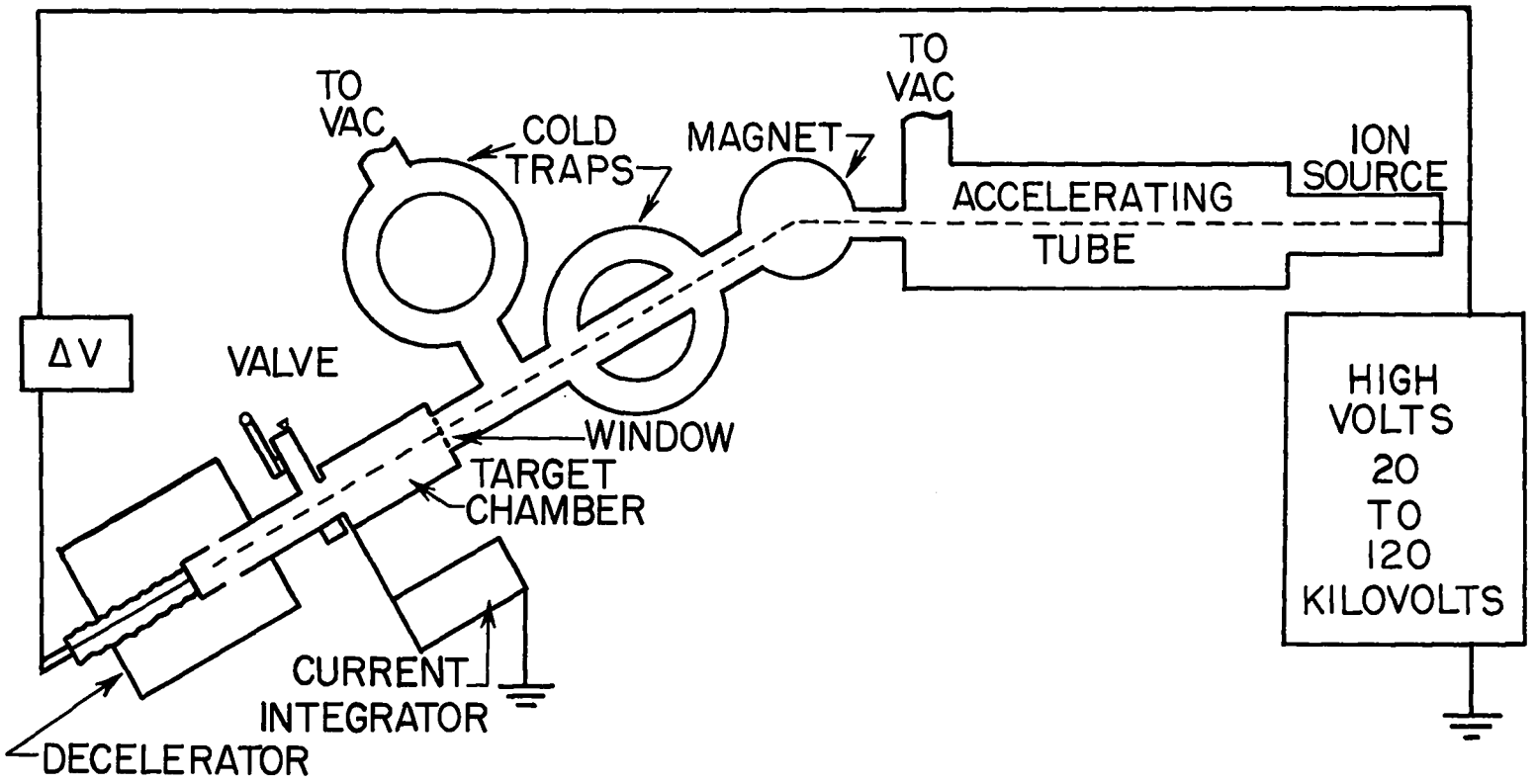

CROSS SECTION APPARATUS

Fig. 1. Cross section apparatus

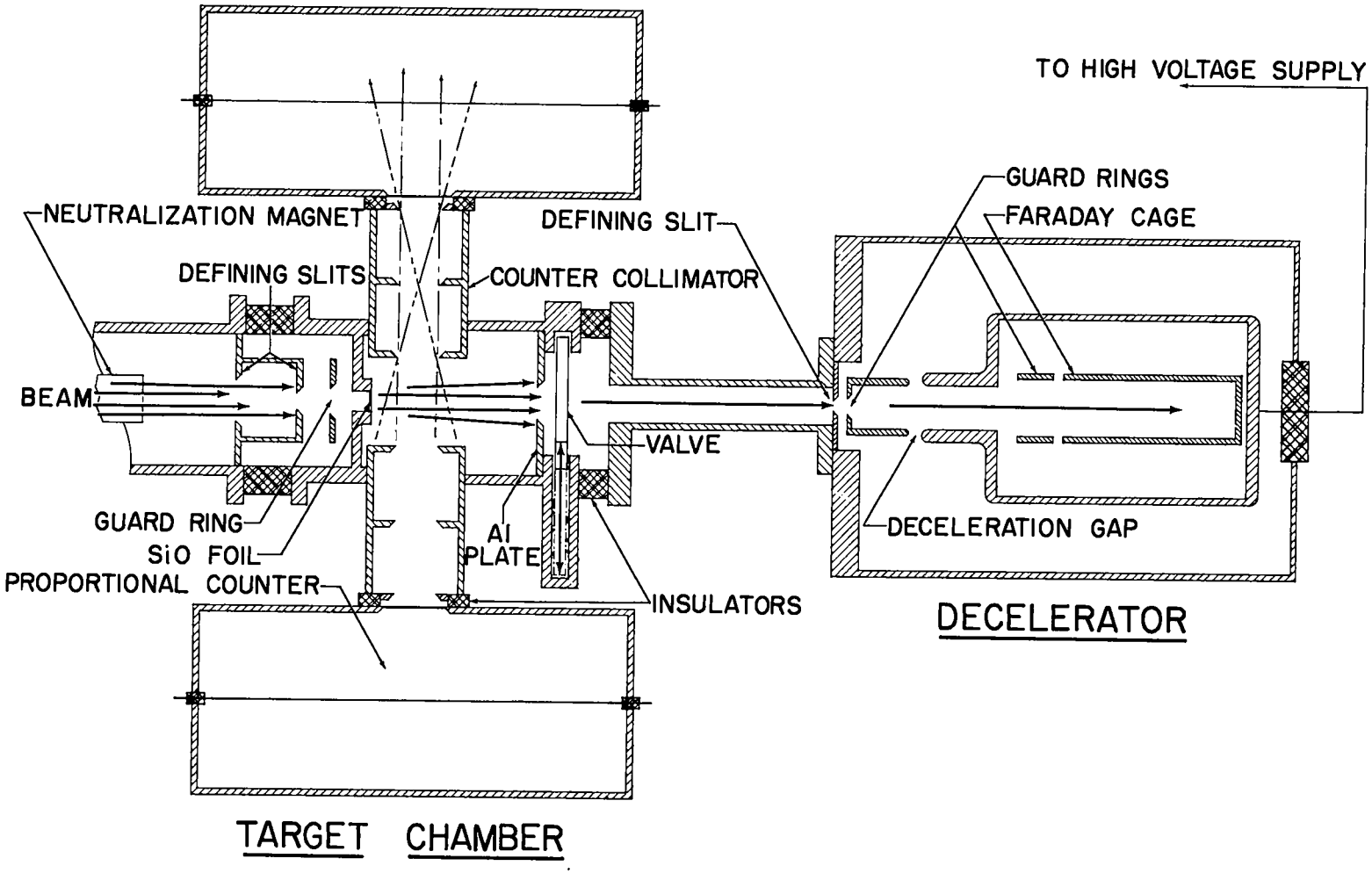

Fig. 2. Target chamber and decelerator for measurement of the T-D cross section

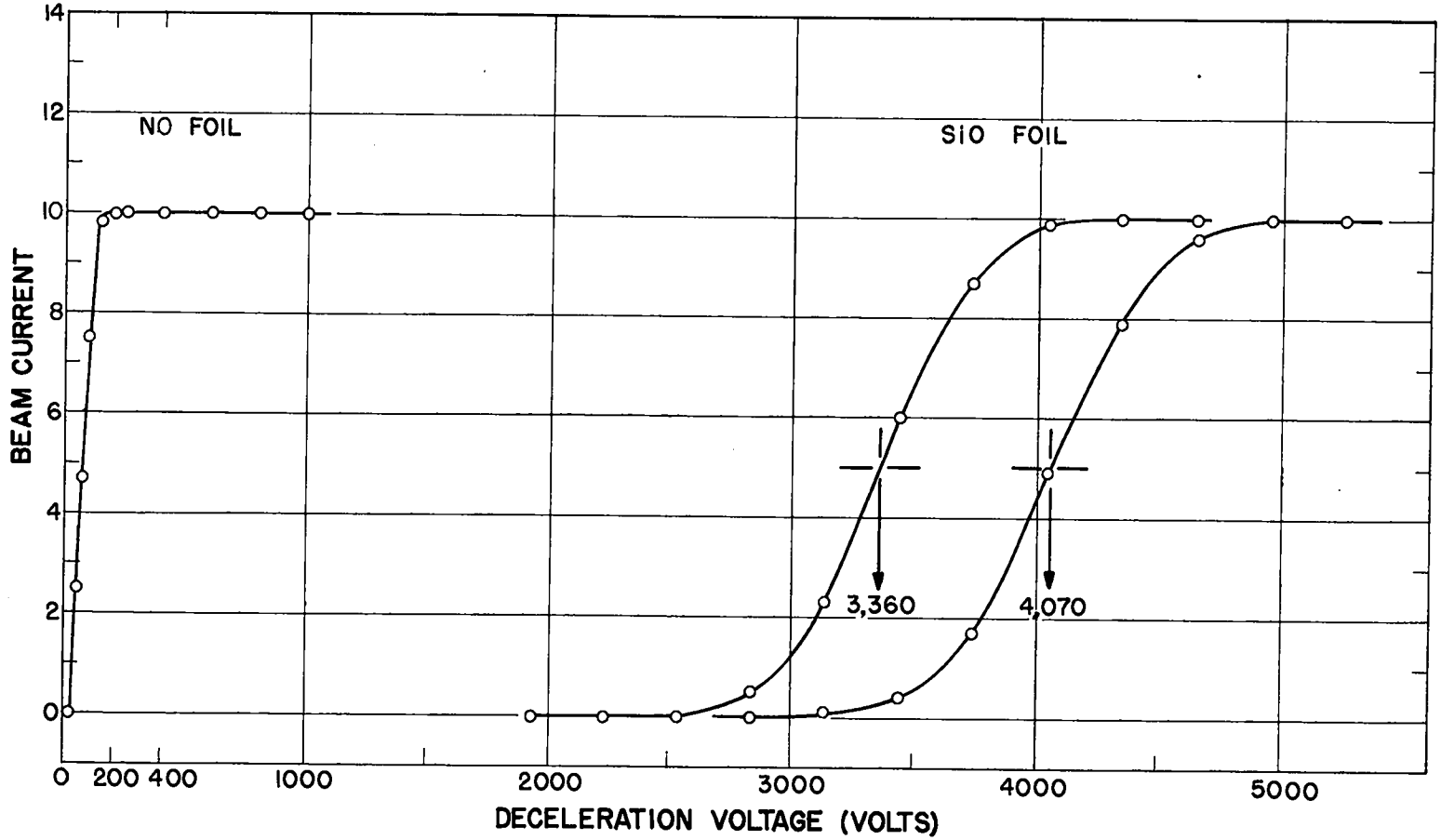

Fig. 3. Typical deceleration curves

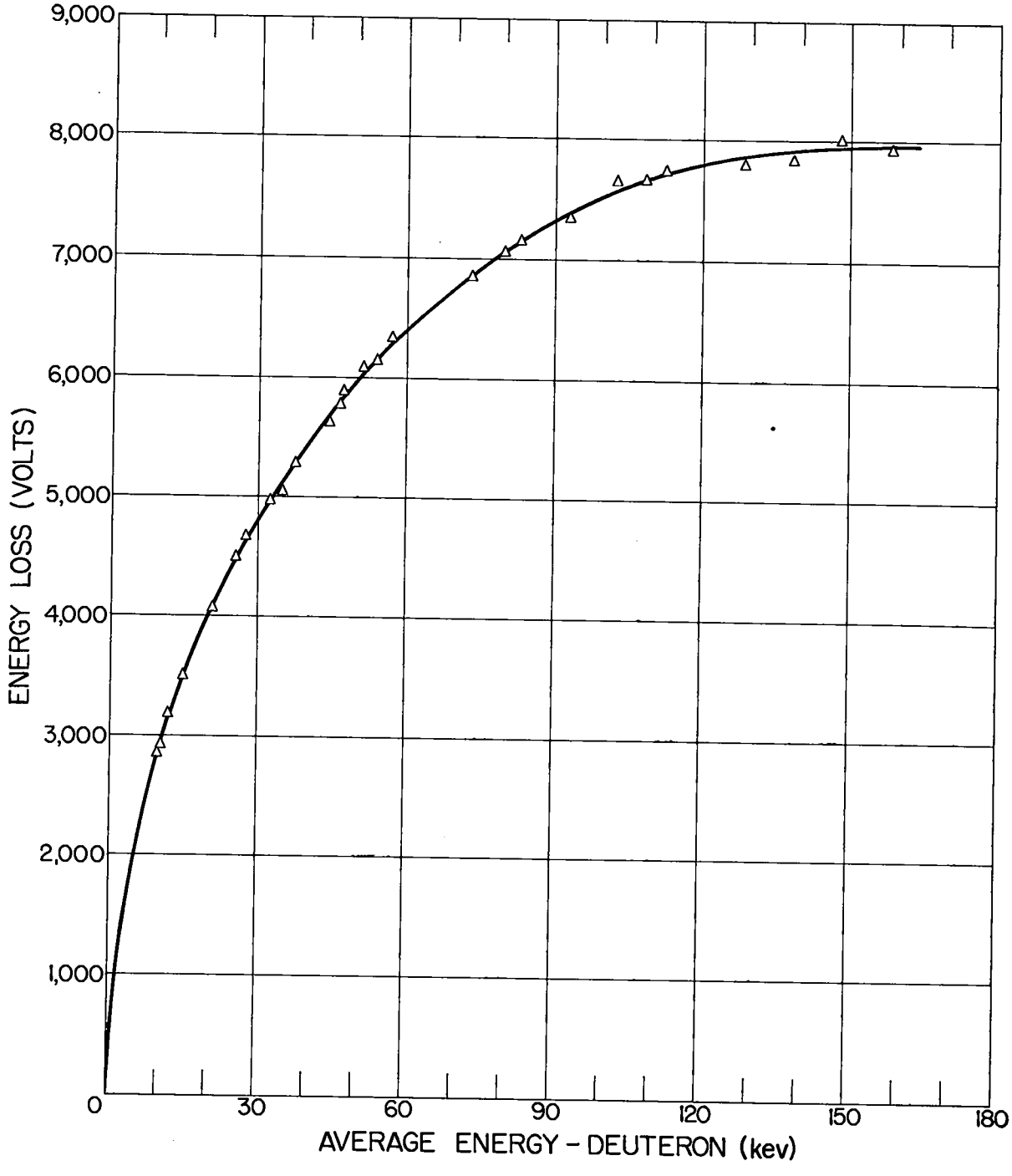

Fig. 4. Energy loss for SiO foils

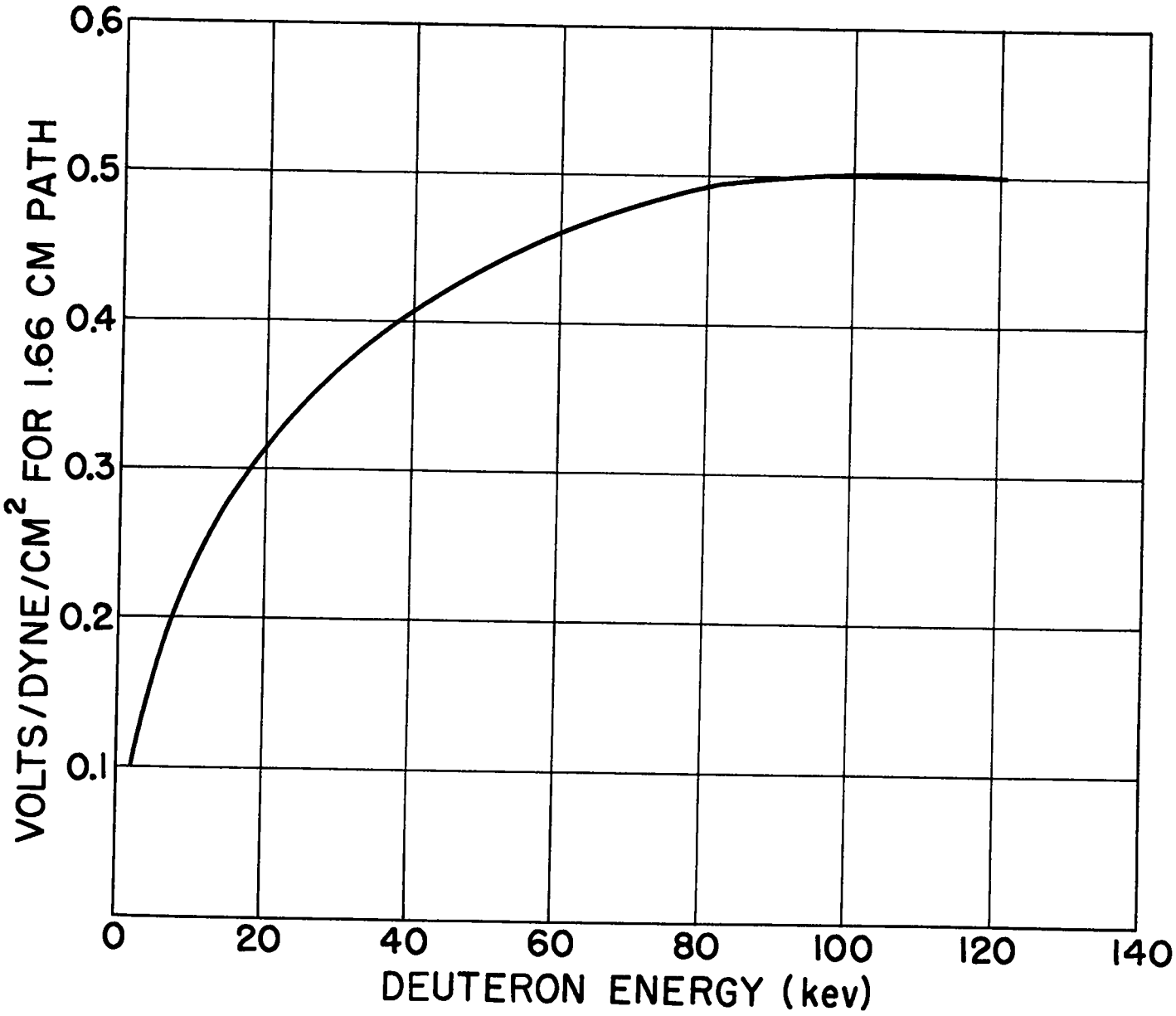

Fig. 5. Energy loss of deuterons in T_2 as a function of energy

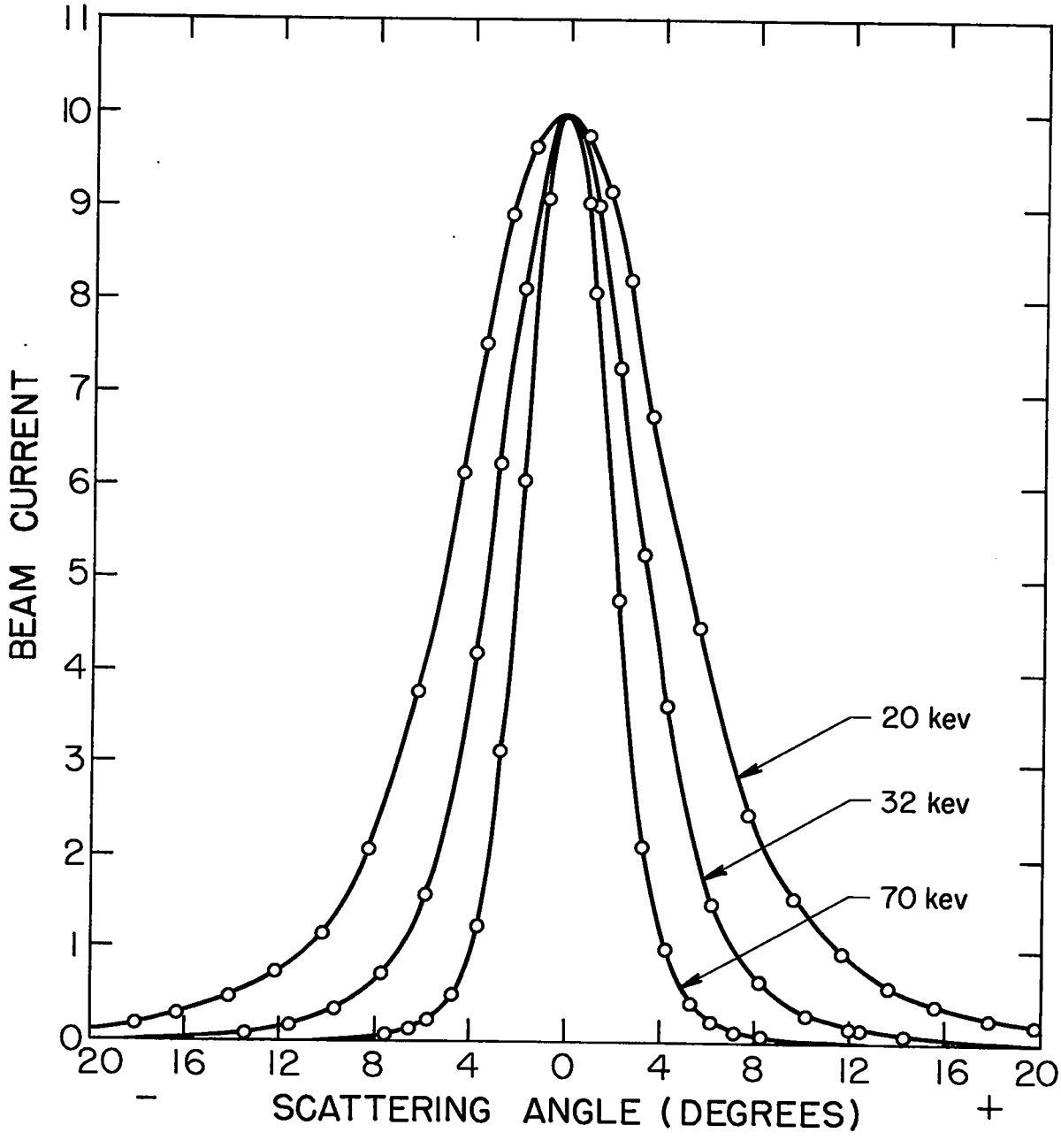

Fig. 6. Scattering in SiO foil

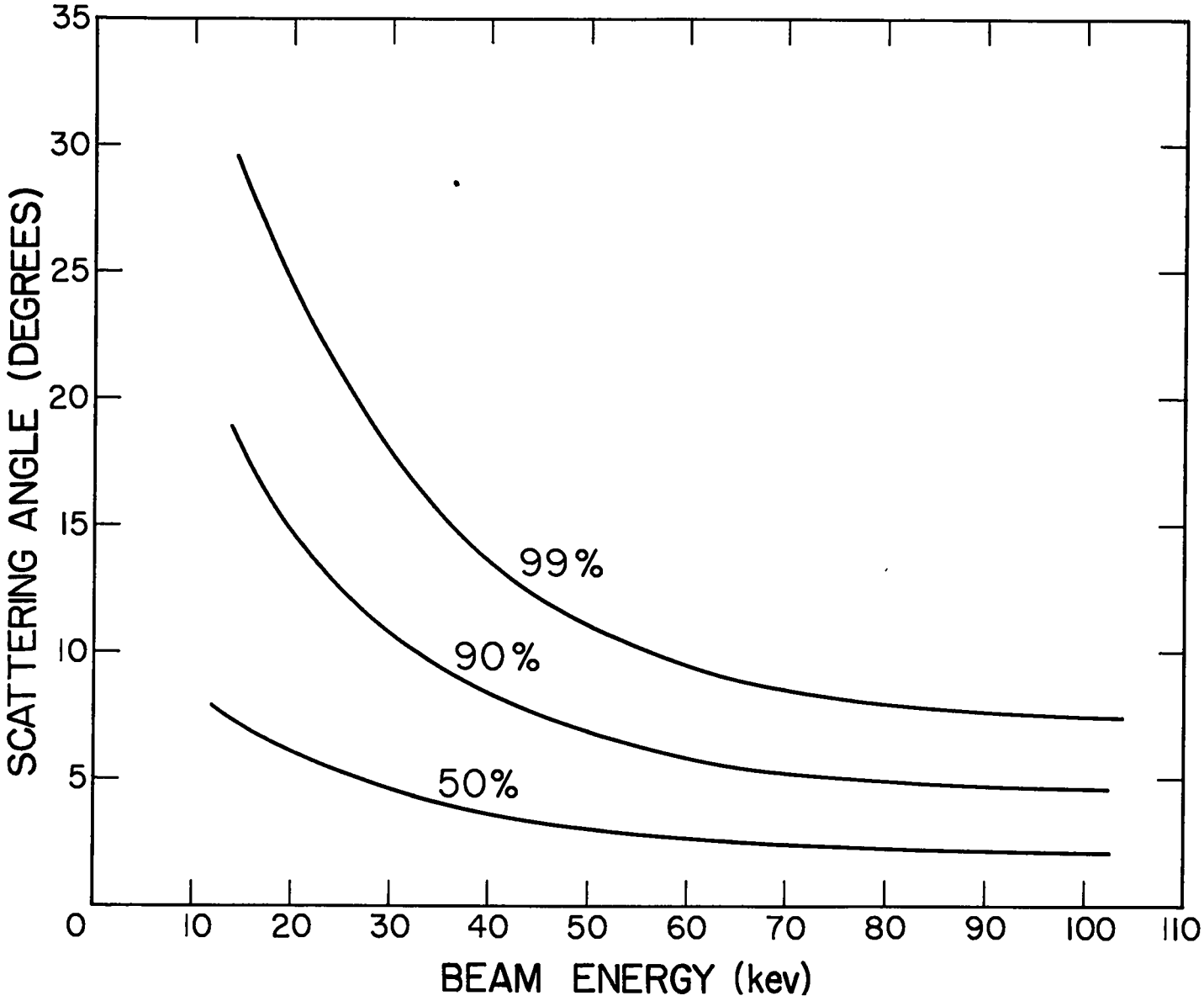

Fig. 7. Angle for inclusion of 50, 90, 99 per cent of total beam vs incident beam energy

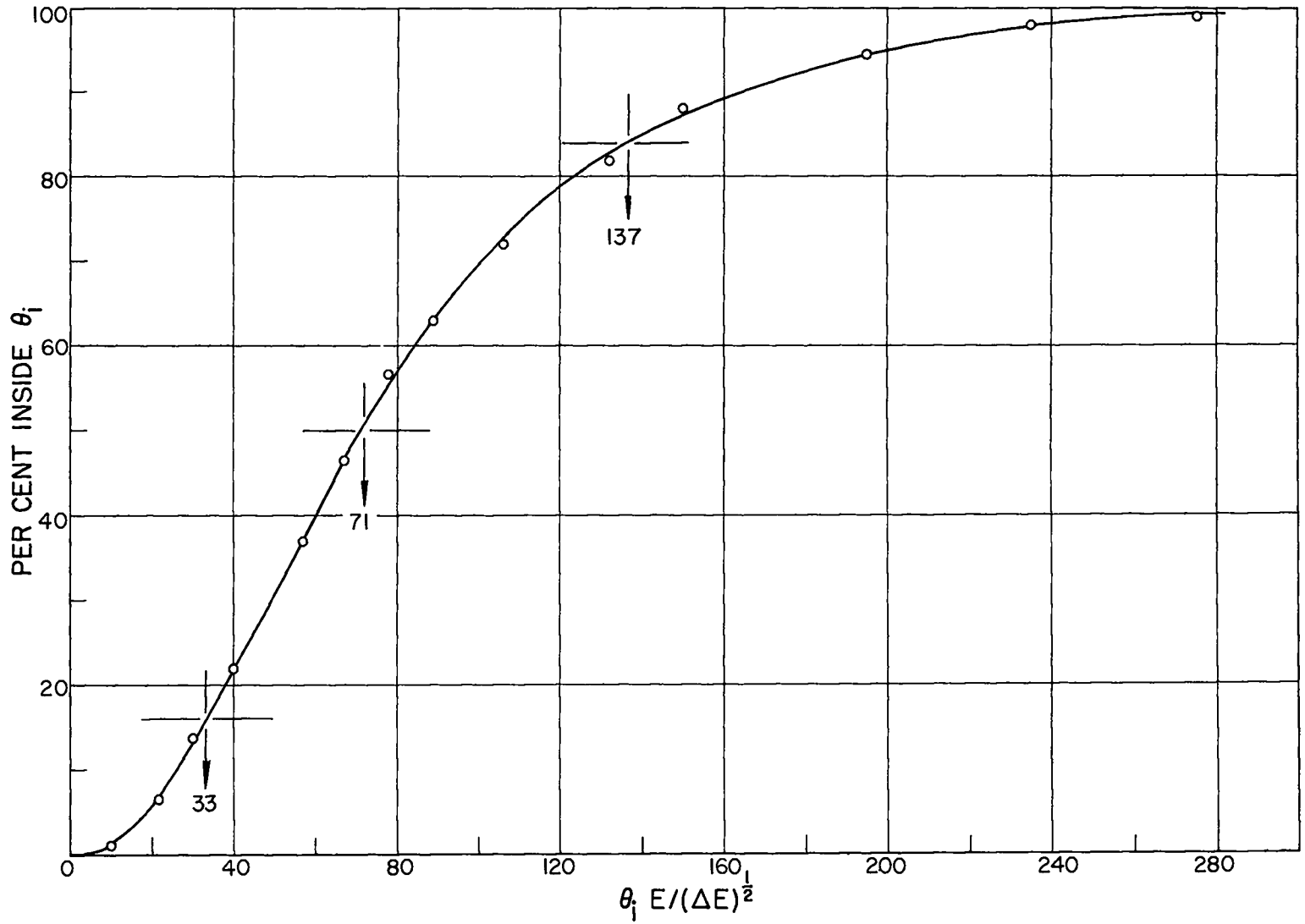

Fig. 8. Per cent of beam included inside angle θ

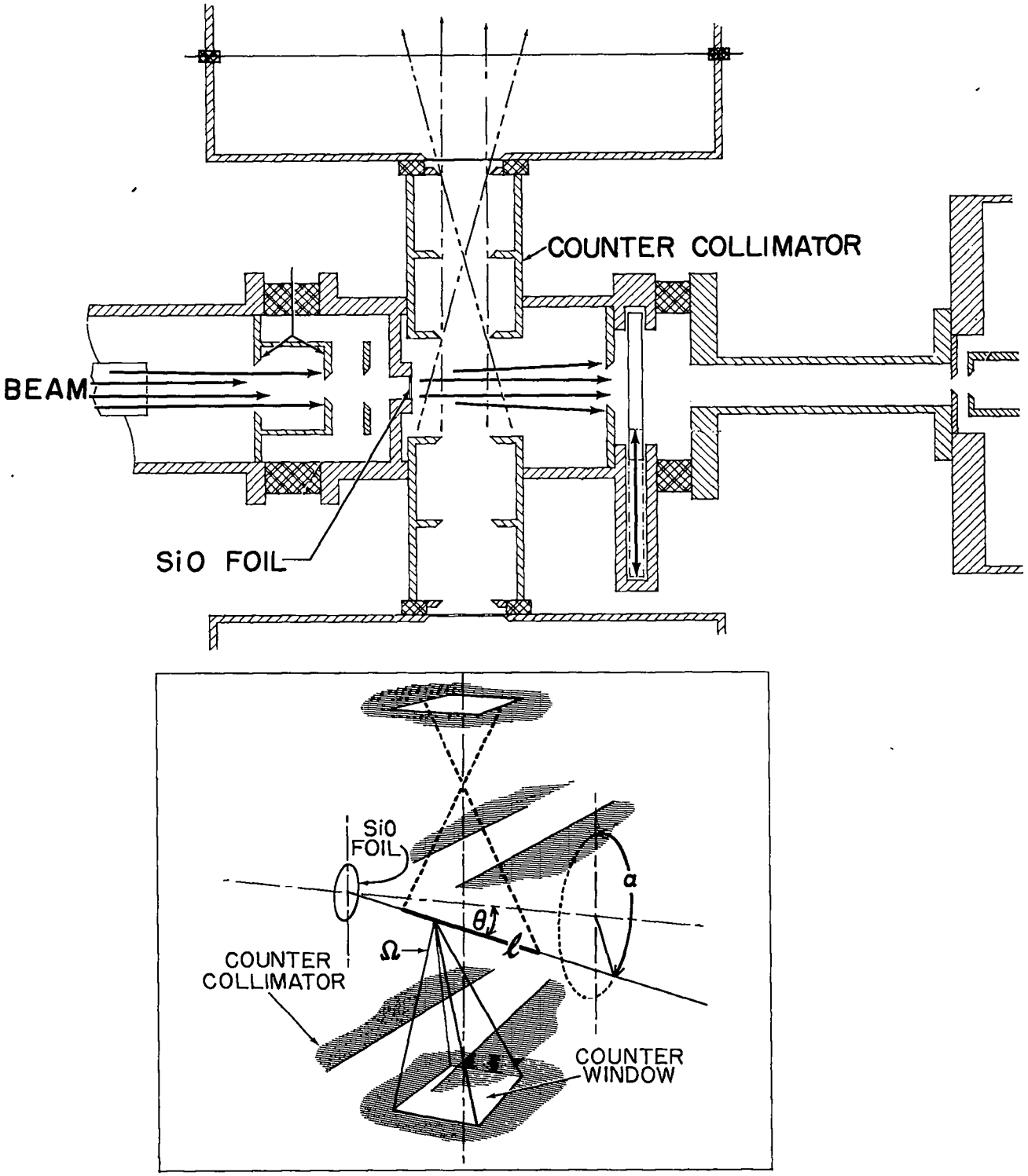

Fig. 9. Schematic diagram of target chamber showing geometry

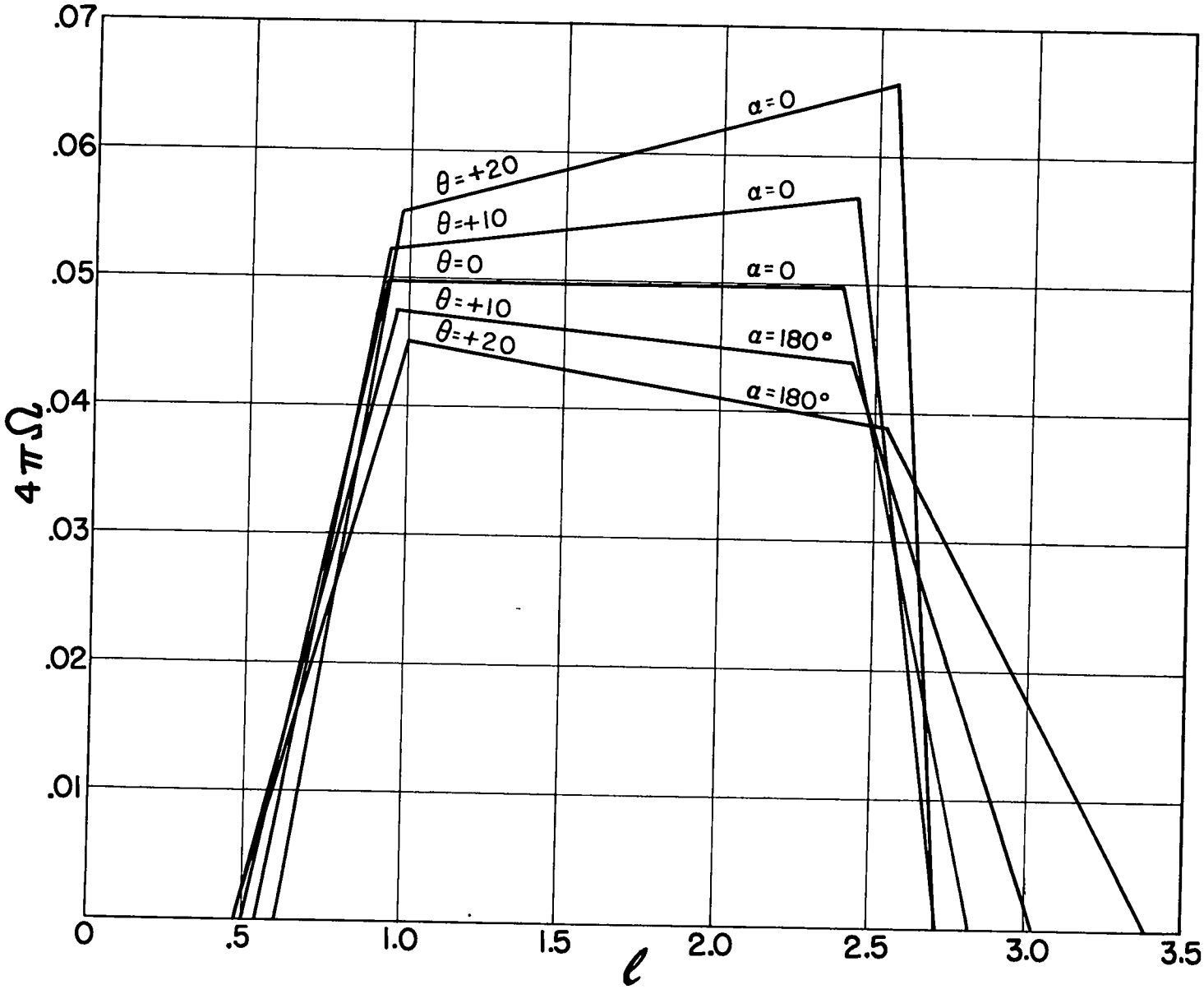

Fig. 10. Solid angle subtended by the counters as a function of distance from the SiO window along the beam for several angles of inclination of beam to axis

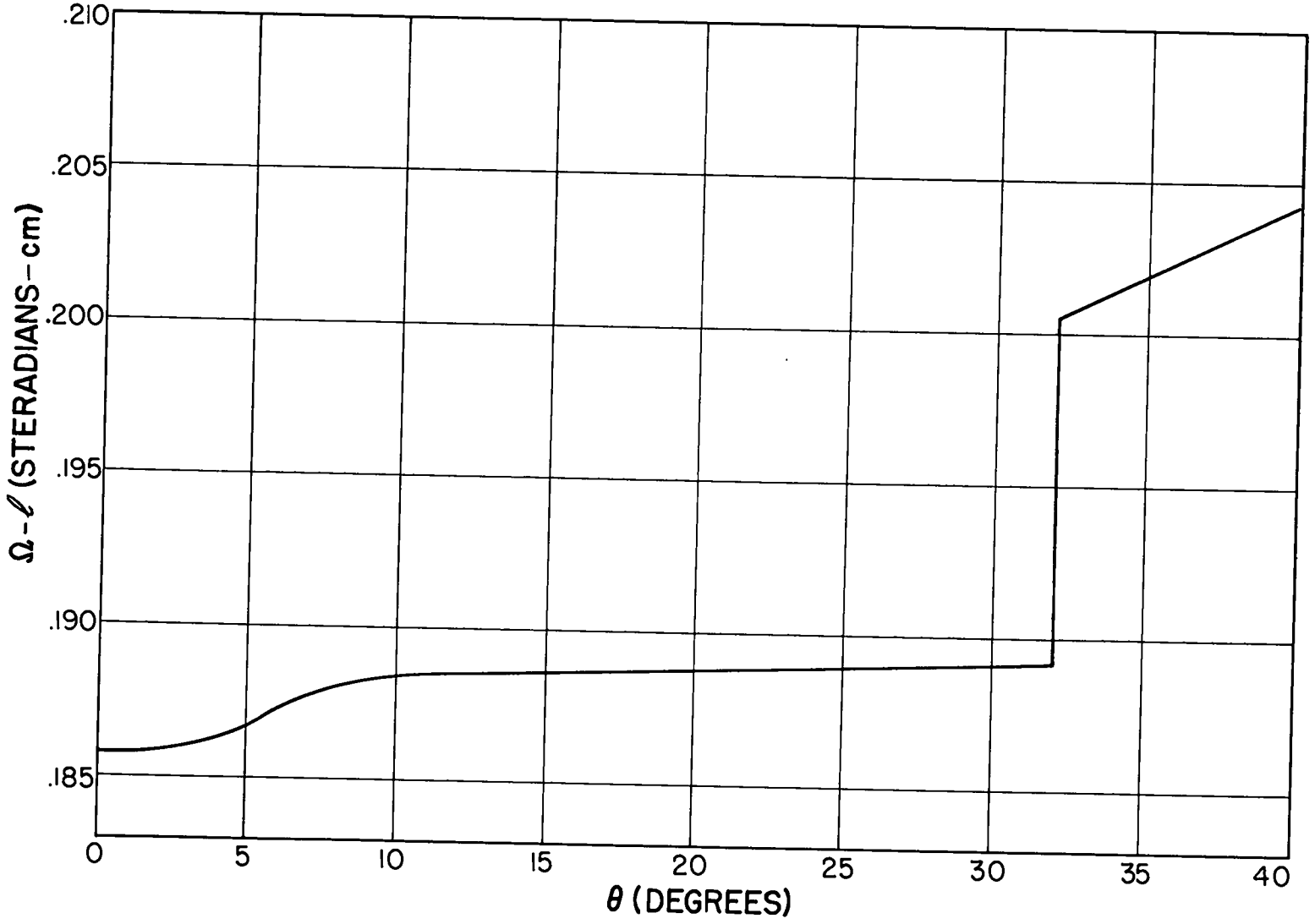

Fig. 11. Product of solid angle subtended by the counters and beam path length as a function of scattering angle

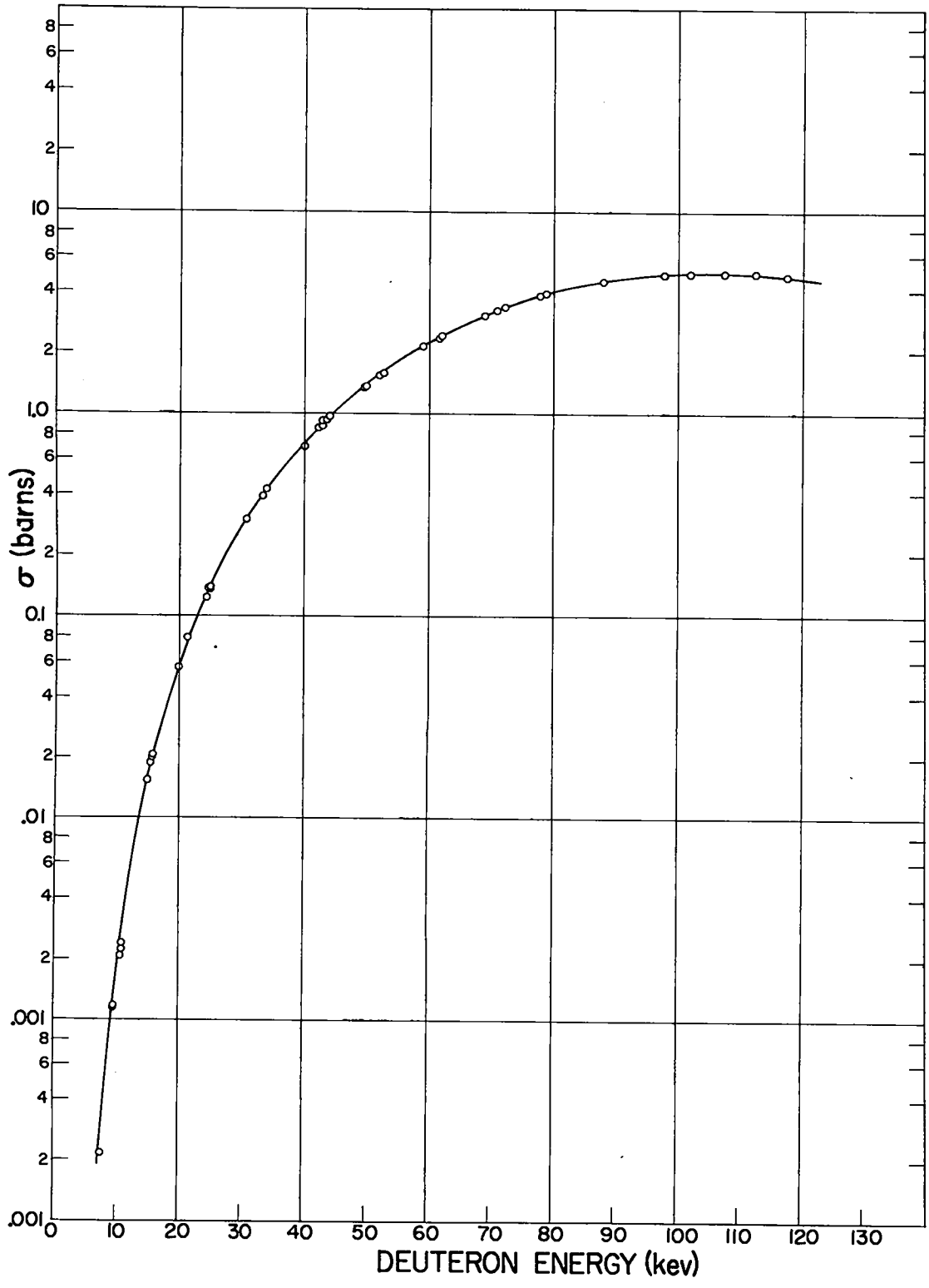

Fig. 12. $T(d,n)He^4$ cross section

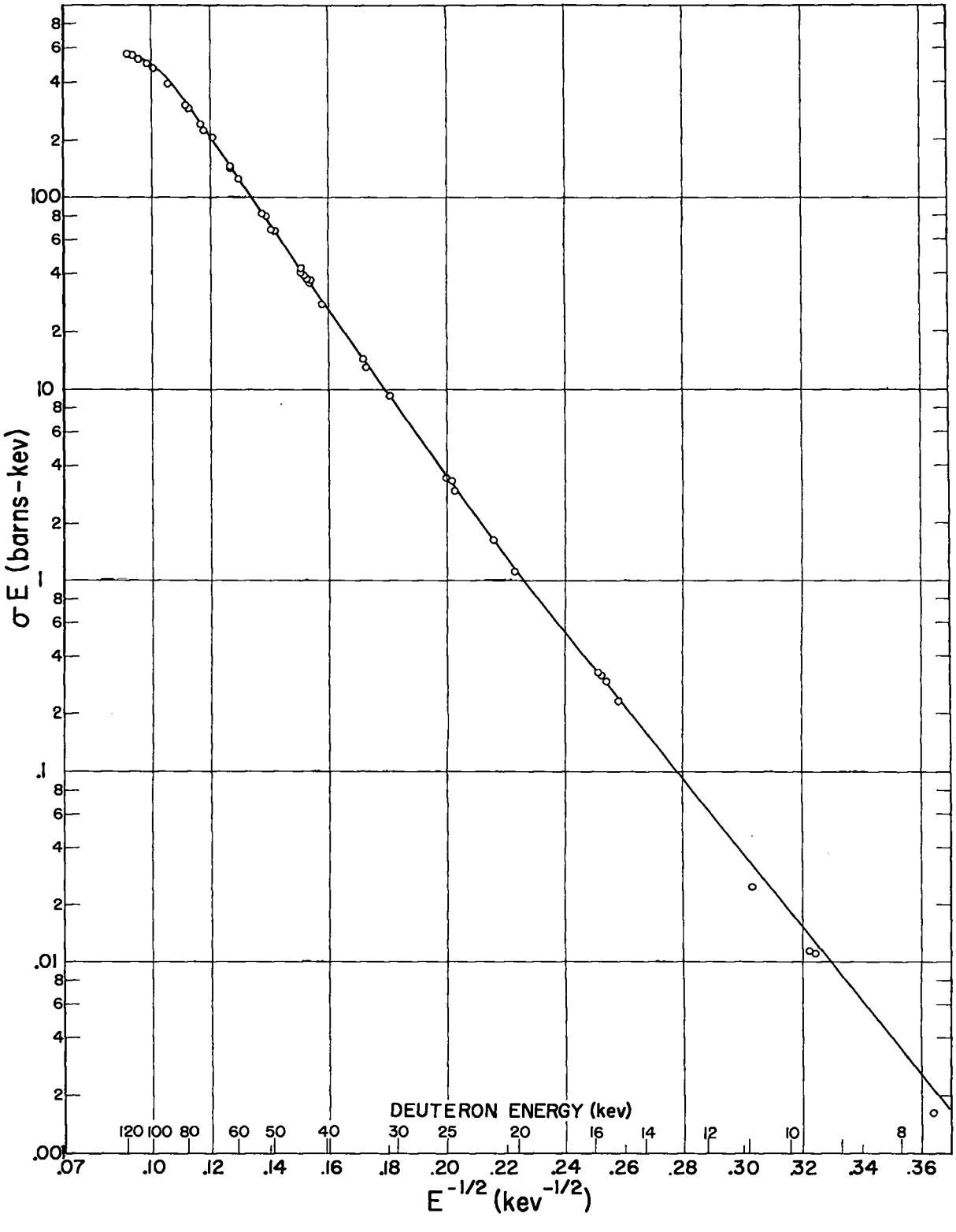

Fig. 13. Gamow plot of cross section $T(d,n)He^4$

REPORT LIBRARY
REC. FROM QL
DATE 1-16-53
RECEIPT ✓